HHS Public Access

Author manuscript

Mamm Genome. Author manuscript; available in PMC 2021 April 06.

Published in final edited form as:

Mamm Genome. 2011 April ; 22(3-4): 170–177. doi:10.1007/s00335-010-9310-6.

A mouse model for human hearing loss DFNB30 due to loss of function of myosin IIIA

Vanessa L. Walsh[#],
Departments of Medicine and Genome Sciences, University of Washington, Seattle, WA 98195-7720, USA

Dorith Raviv[#],
Department of Human Molecular Genetics and Biochemistry, Sackler Faculty of Medicine, Tel Aviv University, Tel Aviv 69978, Israel

Amiel A. Dror,
Department of Human Molecular Genetics and Biochemistry, Sackler Faculty of Medicine, Tel Aviv University, Tel Aviv 69978, Israel

Hashem Shahin,
Department of Biological Sciences, Bethlehem University, Bethlehem, Palestinian Authority

Tom Walsh,
Departments of Medicine and Genome Sciences, University of Washington, Seattle, WA 98195-7720, USA

Moien N. Kanaan,
Department of Biological Sciences, Bethlehem University, Bethlehem, Palestinian Authority

Karen B. Avraham,
Department of Human Molecular Genetics and Biochemistry, Sackler Faculty of Medicine, Tel Aviv University, Tel Aviv 69978, Israel

Mary-Claire King
Departments of Medicine and Genome Sciences, University of Washington, Seattle, WA 98195-7720, USA

[#] These authors contributed equally to this work.

Abstract

The motor protein myosin IIIA is critical for maintenance of normal hearing. Homozygosity and compound heterozygosity for loss-of-function mutations in *MYO3A*, which encodes myosin IIIA, are responsible for inherited human progressive hearing loss DFNB30. To further evaluate this hearing loss, we constructed a mouse model, $Myo3a^{KI/KI}$, that harbors the mutation equivalent to the nonsense allele responsible for the most severe human phenotype. $Myo3a^{KI/KI}$ mice were compared to their wild-type littermates. Myosin IIIA, with a unique N-terminal kinase domain and

M.-C. King, mcking@u.washington.edu.

Electronic supplementary material The online version of this article (doi:10.1007/s00335-010-9310-6) contains supplementary material, which is available to authorized users.

a C-terminal actin-binding domain, localizes to the tips of stereocilia in wild-type mice but is absent in the mutant. The phenotype of the *Myo3a*$^{KI/KI}$ mouse parallels the phenotype of human DFNB30. Hearing loss, as measured by auditory brainstem response, is reduced and progresses significantly with age. Vestibular function is normal. Outer hair cells of *Myo3a*$^{KI/KI}$ mice degenerate with age in a pattern consistent with their progressive hearing loss.

Introduction

Recessive loss-of-function mutations in the molecular motor myosin IIIA are the cause of the human hearing impairment phenotype DFNB30 (Walsh et al. 2002). Myosin IIIA was first identified as NINAC in *Drosophila melanogaster*, where its expression is restricted to the eye photoreceptor cells. Mutations in *NINAC* are associated with abnormal photoreceptor electrophysiology (Montell and Rubin 1988). In mammals, myosin IIIA is expressed in the retina (Dose and Burnside 2000) and inner ear (Schneider et al. 2006; Walsh et al. 2002). Like all proteins in the unconventional myosin superfamily, myosin IIIA consists of a motor head domain, short regulatory neck domain, and a variable tail domain (Friedman et al. 1999). Unlike the other myosins, myosin IIIA is characterized by a distinctive amino terminal kinase domain that undergoes autophosphorylation (Ng et al. 1996). The tail domain is important for phototransduction in *Drosophila* (Porter and Montell 1993) and for actin binding, essential for targeting the protein to filopodia tips in mammalian cells (Les Erickson et al. 2003).

In the mouse inner ear, myosin IIIA is localized at stereocilia tips in a “thimble-like” pattern (Schneider et al. 2006). Stereocilia are actin-rich formations, arranged as staircase-shaped bundles at the apical part of inner-ear hair cells. Stereocilia detect mechanical stimuli by activation of mechanoelectrical channels at the stereocilia tips. Stereocilia formation, hair cell bundle organization, and mechanosensory function depend on several unconventional myosins that when mutant lead to hearing loss.

Homozygosity or compound heterozygosity for any of three different mutations in human *MYO3A* lead to progressive nonsyndromic hearing loss, described in an extended Israeli kindred, Family N, originally from Mosul, Iraq (Walsh et al. 2002). The mutations are a nonsense mutation, 3126T > G, leading to a stop at amino acid 1043 at the C terminus of the motor head, and two splice mutations: 1777(−12)G > A, leading to an out-of-frame deletion of exon 18 and premature protein truncation, and 732(−2)A > G in intron 8, leading to an unstable message.

Mouse models for human hearing impairment have made a dramatic impact on our understanding of the mechanisms involved in this sensory defect (Brown et al. 2008; Dror and Avraham 2009). The relatively short life span of a mouse and therefore rapid development of the inner ear, the striking similarities between the hearing systems of humans and mice, and the accessibility to inner-ear organs in the mouse have facilitated the contribution of this vertebrate model in the field. In this report we describe a mouse model for the loss of function of *MYO3A*.

Materials and methods

Generation of the *Myo3a*$^{KI/KI}$ mouse

All procedures involving animals met NIH guidelines and were approved by the Animal Care and Use Committees of the University of Washington and Tel Aviv University. A modified gene knockout technology was employed to generate targeted embryonic stem (ES) cells and mice chimeric for a nonsense mutation leading to a stop at codon 1041. To generate a suitably modified line of ES cells, we constructed a plasmid vector containing two arms of homology to the *Myo3a* locus (Fig. 1a, b). One arm of homology included the comparable mouse sequence of the human *MYO3A_3126T > G* nonsense mutation, which introduces a stop at codon 1041. The arms of homology were separated by an ACN cassette, kindly provided by Mario Capecchi (Bunting et al. 1999).

Plasmid p4317G9 was used as a vector backbone (Fig. 1b). Into this plasmid was cloned the ACN cassette from pACN to facilitate the subsequent excision of exogenous sequences by Cre-mediated recombination without the need for multiple time-consuming rounds of backcrossing (Bunting et al. 1999). Two regions of homology to the mouse *Myo3a* gene were generated by PCR using primers that included restriction enzyme sites. The first region of homology (5.7 kb long) was subcloned into pBluescript and fully sequenced. A nonsense mutation corresponding to that found in Family N was introduced by site-directed mutagenesis. After confirmation by sequencing, this fragment was cloned into the modified p4317G9 plasmid, upstream of the ACN cassette. The second region of homology (1.7 kb long) was then cloned downstream of the ACN cassette.

Embryonic stem cells of strain C57BL/6 were transfected with clone pVW66 DNA under the positive selection of neomycin and the negative selection of diphtheria toxin. Screening was carried out by PCR with one primer in the ACN cassette and the other in the *Myo3a* gene, beyond the region included in the targeting vector. Of 64 ES cell clones, three correctly targeted clones were obtained. Hemizygosity for the nonsense mutation in the targeted clones was confirmed by site-specific PCR and sequencing, long-range PCR and sequencing, and Southern blot.

Clones were injected into blastocysts of strain Balb/c to generate chimeric mice containing both cells from the host blastocyst (strain Balb/c) and mutant cells of C57BL/6 origin. The use of ES cells derived from strain C57BL/6, rather than strain 129/Ola, allowed for breeding chimeras directly with C57BL/6 mice, which introduced the mutation directly to an inbred background, minimizing subsequent backcrossing.

Genotypes of *Myo3a* homozygous mutant, heterozygous, and wild-type mice were confirmed by sequencing genomic DNA from intron 27 to exon 28 using primers flanking the site of the mutation: F 5′-GCATAGAGCCTTCATAGG-3′ and R 5′-TTGGTGATTACCTGACTG-3′. To confirm *Myo3a* message sequence, RNA was isolated from the cochlea of mice of each genotype and the RT-PCR products were directly sequenced using primers in exons 27 and 28, which flanked a splice site and the putative stop codon.

Myo3a$^{KI/KI}$ mice are available through The Jackson Laboratory (JAX stock number 14165).

Measurement of hearing thresholds

Hearing thresholds were evaluated with auditory brainstem responses (ABRs) recorded in response to tone bursts, as described previously (McCullough and Tempel 2004). Evaluations were carried out on mice aged 2.5, 5, 7.5, 10, and 13 months. Anesthetized mice were placed in a sound-attenuating chamber. Body temperature was maintained at approximately 37°C by an isothermal heating pad (Braintree Scientific). Evoked responses were recorded via subdermal needle electrodes placed midline above the frontal bone (positive) and behind the left pinna, with a ground electrode in the left thigh. The system (#2530, Larson-Davis) was calibrated on each day of use with the microphone tip placed at the location of the mouse head. Auditory thresholds were determined by delivering pure tone auditory stimuli (tone bursts) binaurally at 5.6, 8, 11.3, 16, 32, and 40 kHz. Tone-burst stimuli of alternating polarity were repeated at 75-ms intervals in 10-dB increments starting at 90 dB and decreasing to 20 dB. ABRs were recorded over 40 msec and averaged at each intensity level for 1024 presentations. Potentials were amplified (1000×), filtered (0.3–3 kHz) by a preamplifier (P55, Grass-Telefactor), and digitized. Thresholds were determined visually as the lowest SPL (in 5-dB increments) in which a recognizable waveform was present and repeatable. At each age, *Myo3a* mutant mice were compared to their wild-type littermates.

Vestibular tests

Clinical ocular motor and vestibular examination included eye movement testing, evaluation of spontaneous nystagmus with and without visual fixation, evaluation of dynamic vestibulo-ocular reflex (VOR) function, and positioning test for posterior and horizontal canal benign paroxysmal positional vertigo (BPPV) (Zee and Fletcher 1996). Vestibular studies in humans were approved by the Helsinki Committees of Tel Aviv University and the Israel Ministry of Health and the Institutional Review Board of the University of Washington (protocol 33468). To evaluate vestibular function in the *Myo3a* mutant mice, behavior of mutant mice was compared to their wild-type littermates using the modified SHIRPA protocol of reaching response and swim tests (Green et al. 2005).

Immunohistochemistry

Affinity-purified rabbit polyclonal antibody MyoIIIa-NPYD was custom-made (Sigma) against a synthetic peptide (NPYDYRRLLRKTSQRQR) that matches the C-terminus sequence of the mouse myosin IIIA. For validation of the antibody, HEK293T cells were transfected with a pFlag-myosin IIIA construct that expresses the tail portion (amino acids 1079–1614) of myosin IIIA. Cells were lysed and run on an SDS-PAGE gel, followed by Western blot analysis with anti-myosin IIIA, and compared to cells transfected with a pFlag empty vector.

For immunohistochemistry, cochleae were prepared as previously described (Hertzano et al. 2008). Antigen retrieval was achieved by incubating 30 min at 60°C in 0.1 M citrate buffer with 0.05% Tween-20, pH 7, followed by blocking in 10% normal donkey serum and 1% BSA in PBS for 1 h at room temperature. Samples were labeled with primary antibody

overnight at 4°C, washed, and then counterstained with fluorescent conjugated secondary antibody (Alexa-Fluor® 488, Molecular Probes). Rhodamine phalloidin was used to visualize the stereocilia F-actin. Samples were visualized using a Zeiss LSM 510 confocal microscope.

Scanning electron microscopy

Inner ears of adult mice were dissected and prepared as previously described (Hertzano et al. 2008). Samples were prepared according to the osmium tetroxide-thiocarbohydrazide (OTOTO) method (Self et al. 1998). Samples were than transferred to critical point dry and gold coating procedure and scanned using JSM 840A scanning electron microscope (Jeol).

Hair cell counts

Outer-hair-cell (OHC) degeneration was evaluated by counting the number of normal cells and the number of degenerating cells in montages of scanning electron micrographs of the organ of Corti. Three mice of each genotype were evaluated. For each sample, 10–12 adjacent images were taken at 1000× magnification (showing approximately 60 OHC per image), from the apical area toward the basilar turn, completing one full turn of the cochlea. OHC counting began where the cochlea completes approximately one full turn. OHC in regions ranging from 30 to 90% of the distance from the base of the cochlea were analyzed, corresponding to frequencies of approximately 36.5–5.4 kHz (Taberner and Liberman 2005). Inner hair cells (IHC) could not be counted consistently because residues of Reissner's membrane covered the IHC in many areas. Proportions of OHC present at comparable frames and ages of *Myo3a*$^{KI/KI}$ mice versus their wild-type littermates were evaluated using χ^2 tests with Yates' corrections.

Results

Progressive hearing loss of *Myo3a*$^{KI/KI}$ mice

We generated the *Myo3a*$^{KI/KI}$ mouse to serve as a model for human progressive hearing loss DFNB30 (Walsh et al. 2002), by introducing the nonsense mutation TAT > TAG at codon 1041 of mouse myosin IIIA (Fig. 1a, b). The sequence in this region is conserved between human and mouse, with the corresponding human mutation at codon 1042. Sequencing cDNA from *Myo3a*$^{KI/KI}$, heterozygous, and wild-type mice confirmed the expected nucleotide at exon 28 in all three genotypes. Sequence for the homozygous mutant mouse is shown in Fig. 1c.

Hearing thresholds in mutant and wild-type mice are illustrated in Fig. 2 and given Supplementary Table 1. Hearing loss of *Myo3a*$^{KI/KI}$ mice is significant and progressive. In mutant mice, hearing loss is significant at 2.5 months and progresses first at high frequencies, then at all frequencies. Differences between *Myo3a*$^{KI/KI}$ and wild-type mice are significant at middle frequencies as late as 13 months.

Normal vestibular function of *Myo3a*$^{KI/KI}$ mice and of DFNB30 humans

Auditory defects are frequently associated with vestibular defects. Furthermore, myosin IIIA is expressed in the vestibular hair cells (Schneider et al. 2006). *Myo3a*$^{KI/KI}$ mice were tested

for vestibular abnormalities based on reaching response and forced swimming abilities and were normal (Supplementary Fig. 1).

Individuals in Family N with hearing loss had not described any balance defects (Walsh et al. 2002). A profoundly deaf member of Family N, subject IV:2, was evaluated. Subject IV:2 is male, age 57, and homozygous for the nonsense mutation *MYO3A c.3126T > G*. All of his ocular motor and vestibular examinations were normal, including eye movement testing, evaluation of spontaneous nystagmus with and without visual fixation, evaluation of dynamic VOR function, and positioning test for posterior and horizontal canal BPPV.

Localization of myosin IIIA to stereocilia tips of inner and outer hair cells in wild-type mice

The mouse inner ear, similar to the human structure, contains a sensory epithelium that is made up of three rows of outer hair cells and one row of inner hair cells (Fig. 3a). The hair bundle lies on the apical portion of the hair cells, on the cuticular plate, and is composed of stereocilia containing crosslinked actin filaments. The specificity of the MyoIIIa-NPYD antibody, made to the C-terminal part of the protein, was validated by transfection of HEK293T cells with the construct expressing pFlag-MyoIIIa tail portion (Fig. 3b). The MyoIIIa-NPYD antibody detected only myosin IIIa in transfected cells. In wild-type mice, myosin IIIa was detected with the MyoIIIa-NPYD antibody in the stereocilia tips of both inner and outer hair cells (Fig. 3c, e), in all the stereocilia rows, identical to the pattern previously reported (Salles et al. 2009; Schneider et al. 2006). As expected, in $Myo3a^{KI/KI}$ mice, no myosin IIIA was detectable by the MyoIIIa-NPYD antibody (Fig. 3d, f).

Outer-hair-cell degeneration in $Myo3a^{KI/KI}$ mice

The mouse inner ear, similar to the human structure, contains sensory epithelium that is made up of three rows of OHCs and one row of IHCs (Fig. 3). Based on scanning electron microscopy of the inner ear, at 8 days, 6 months, and 8.5 months stereocilia hair bundles of mutant mice were shaped normally, with a well-organized stereocilia staircase, compared to wild-type littermates. By 10 and 17 months, both IHCs and OHCs demonstrated signs of degeneration (Fig. 4a-h).

In contrast to the normal morphology of individual hair bundles, fewer hair cells were present in $Myo3a^{KI/KI}$ mice than in wild-type mice. Degenerative changes, reflected by loss of OHCs, were significant in the $Myo3a^{KI/KI}$ mice. At 10 months, loss of OHC was more severe for $Myo3a^{KI/KI}$ mice than for their wild-type littermates across all regions of the cochlea (Fig. 4i). At the midcochlear turn, OHC loss was more severe for $Myo3a^{KI/KI}$ than wild-type mice beginning at 10 months and continuing to old age (Fig. 4j). The midcochlear turn, approximately 70% of the distance from the base of the cochlea, corresponds to received sound frequencies of 11.3 kHz, where hearing loss of the $Myo3a^{KI/KI}$ mice is most pronounced (Fig. 2).

Discussion

$Myo3a^{KI/KI}$ mice, with a nonsense mutation characteristic of human DFNB30, exhibit progressive recessive hearing loss, closely reflecting the hearing loss of Family N. Examination of the cochlea of $Myo3a^{KI/KI}$ mice revealed patterns of loss of OHCs at ages

and cochlear regions concordant with their hearing impairment. Degeneration of OHCs was observed at 10 months and older. Hair cell loss was greater toward the base, reflecting the more severe hearing loss at higher frequencies. The pattern of OHC loss paralleled the pattern of hearing loss in the human DFNB30 family.

It is intriguing that humans and mice with myosin IIIA-related hearing loss have normal vestibular function, despite localization of myosin IIIA to both cochlear and vestibular hair cells (Schneider et al. 2006). Similarities to *Cdh23*$^{ahl/ahl}$ mice, which have hearing loss and normal balance (Noben-Trauth et al. 2003), may resolve this paradox. OHCs toward the base of the cochlea have more stereocilia than do vestibular hair cells (Lim 1986). Thu, loss of cadherin 23, which is localized to stereocilia tips, may confer greater damage to more basal cochlear hair cells than to vestibular hair cells. In *Cdh23*$^{ahl/ahl}$ mice, this distinction is reflected in more severe hearing loss at high frequencies (Johnson et al. 2010). The same differential distribution of stereocilia in basal OHCs compared to vestibular hair cells may explain the combination of hearing loss and normal vestibular function for Family N individuals and *Myo3a*$^{KI/KI}$ mice. Alternatively, other myosins may compensate for myosin IIIA loss in vestibular hair cells.

Hair cell morphology in mouse mutants with hearing impairment appears to follow one of two paths: severe hair cell disorganization followed by degeneration and loss of hair cells and spiral ganglion cells, or, alternatively, hair cell degeneration with subtle prior structural alterations. *Myo3a*$^{KI/KI}$ mutant mice follow the latter pattern. Structural changes such as fused stereocilia and disorganized hair bundles may be due to primary effects of mutations in genes required for bundle cohesion and organization, as in the case of deaf circler (*dfcr*) mice with mutations in harmonin (Johnson et al. 2003). Alternatively, functional changes may be secondary effects in hair cells, as is characteristic of hurry-scurry (*hscy*) mice with *Tmhs* mutations (Longo-Guess et al. 2005) and samba mice with *Loxhd1* mutations (Grillet et al. 2009). In contrast, Beethoven (*Bth*) mice, with *Tmc1* mutations, are more similar to *Myo3a* mice, with relatively intact hair bundles prior to hair cell loss (Vreugde et al. 2002). In such mutants, damage to hair cells may be due to intrinsic or extrinsic factors. For example, for *Cldn14*$^{-/-}$ mutant mice, OHC death appears to be due to extracellular factors (Ben-Yosef et al. 2003).

We speculate that in the case of *Myo3a*$^{KI/KI}$ mice, loss of function of myosin IIIA affects the mechanotransduction process, leading to loss of activity and subsequent degeneration of hair cells. The distinctive thimble-like expression pattern of myosin IIIA at the stereocilia tip (Schneider et al. 2006 and Fig. 3) and the overexpression of myosin IIIA and espin-1 resulting in enhanced elongation of stereocilia (Salles et al. 2009) suggest that myosin IIIA has a role in transporting essential components to the positive end of stereocilia. Given that stereocilia tips are the site for mechanotransduction (Gillespie and Muller 2009), loss of myosin IIIA at this site may lead to loss of mechanotransduction activity. However, recent studies have suggested that transducer channels are in the second and third rows of hair cells, but not the first (Beurg et al. 2009), whereas myosin IIIA appears to be present in all rows of hair cells.

In summary, *Myo3a*$^{KI/KI}$ mice are a genetic model for adult-onset human hearing loss DFNB30. Hearing loss in the mutant mouse is progressive, affecting first high frequencies then the entire frequency range, reflecting the human phenotype. The anatomic correlate of the hearing loss in the *Myo3a*$^{KI/KI}$ mice is degeneration of outer hair cells, which progresses with age and is particularly acute at frequencies at which hearing loss is most severe.

Supplementary Material

Refer to Web version on PubMed Central for supplementary material.

Acknowledgments

We thank members of Family N for their continuous participation in our study. This work was supported by NIH grant R01DC005641 from the National Institute of Deafness and Communication Disorders. We thank Mario Capecchi for the ACN cassette; Richard Palmiter for plasmid p4317G9; Carlos Gordon for vestibular testing; and Yehoash Raphael, Edwin Rubel, Carol Ware, Carol Robbins, Bob Hunter, and Glenn MacDonald for technical help and advice.

References

Ben-Yosef T, Belyantseva IA, Saunders TL, Hughes ED, Kawamoto K et al. (2003) Claudin 14 knockout mice, a model for autosomal recessive deafness DFNB29, are deaf due to cochlear hair cell degeneration. Hum Mol Genet 12:2049–2061 [PubMed: 12913076]

Beurg M, Fettiplace R, Nam J-H, Ricci AJ (2009) Localization of inner hair cell mechanotransducer channels using high-speed calcium imaging. Nat Neurosci 12:553–558 [PubMed: 19330002]

Brown SD, Hardisty-Hughes RE, Mburu P (2008) Quiet as a mouse: dissecting the molecular and genetic basis of hearing. Nat Rev Genet 9:277–290 [PubMed: 18283275]

Bunting M, Bernstein KE, Greer JM, Capecchi MR, Thomas KR (1999) Targeting genes for self-excision in the germ line. Genes Dev 13:1524–1528 [PubMed: 10385621]

Dose AC, Burnside B (2000) Cloning and chromosomal localization of a human class III myosin. Genomics 67:333–342 [PubMed: 10936054]

Dror AA, Avraham KB (2009) Hearing loss: mechanisms revealed by genetics and cell biology. Annu Rev Genet 43:411–437 [PubMed: 19694516]

Friedman TB, Sellers JR, Avraham KB (1999) Unconventional myosins and the genetics of hearing loss. Am J Med Genet 89:147–157 [PubMed: 10704189]

Gillespie PG, Muller U (2009) Mechanotransduction by hair cells: models, molecules, and mechanisms. Cell 139:33–44 [PubMed: 19804752]

Green EC, Gkoutos GV, Lad HV, Blake A, Weekes J et al. (2005) EMPReSS: European mouse phenotyping resource for standardized screens. Bioinformatics 21:2930–2931 [PubMed: 15827082]

Grillet N, Schwander M, Hildebrand MS, Sczaniecka A, Kolatkar A et al. (2009) Mutations in LOXHD1, an evolutionarily conserved stereociliary protein, disrupt hair cell function in mice and cause progressive hearing loss in humans. Am J Hum Genet 85:328–337 [PubMed: 19732867]

Hertzano R, Shalit E, Rzadzinska AK, Dror AA, Song L et al. (2008) A Myo6 mutation destroys coordination between the myosin heads, revealing new functions of myosin VI in the stereocilia of mammalian inner ear hair cells. PLoS Genet 4:e1000207 [PubMed: 18833301]

Johnson KR, Gagnon LH, Webb LS, Peters LL, Hawes NL et al. (2003) Mouse models of USH1C and DFNB18: phenotypic and molecular analyses of two new spontaneous mutations of the *Ush1c* gene. Hum Mol Genet 12:3075–3086 [PubMed: 14519688]

Johnson KR, Yu H, Ding D, Jiang H, Gagnon LH et al. (2010) Separate and combined effects of *Sod1* and *Cdh23* mutations on age-related hearing loss and cochlear pathology in C57BL/6J mice. Hear Res 268:85–92 [PubMed: 20470874]

Les Erickson F, Corsa AC, Dose AC, Burnside B (2003) Localization of a class III myosin to filopodia tips in transfected HeLa cells requires an actin-binding site in its tail domain. Mol Biol Cell 14:4173–4180 [PubMed: 14517327]

Lim DJ (1986) Functional structure of the organ of Corti: a review. Hear Res 22:117–146 [PubMed: 3525482]

Longo-Guess CM, Gagnon LH, Cook SA, Wu J, Zheng QY et al. (2005) A missense mutation in the previously undescribed gene *Tmhs* underlies deafness in hurry-scurry (**hscy**) mice. Proc Natl Acad Sci U S A 102:7894–7899 [PubMed: 15905332]

McCullough BJ, Tempel BL (2004) Haplo-insufficiency revealed in deafwaddler mice when tested for hearing loss and ataxia. Hear Res 195:90–102 [PubMed: 15350283]

Montell C, Rubin GM (1988) The Drosophila *ninaC* locus encodes two photoreceptor cell specific proteins with domains homologous to protein kinases and the myosin heavy chain head. Cell 52:757–772 [PubMed: 2449973]

Ng KP, Kambara T, Matsuura M, Burke M, Ikebe M (1996) Identification of myosin III as a protein kinase. Biochemistry 35:9392–9399 [PubMed: 8755717]

Noben-Trauth K, Zheng QY, Johnson KR (2003) Association of cadherin 23 with polygenic inheritance and genetic modification of sensorineural hearing loss. Nat Genet 35:21–23

Porter JA, Montell C (1993) Distinct roles of the Drosophila ninaC kinase and myosin domains revealed by systematic mutagenesis. J Cell Biol 122:601–612 [PubMed: 8335687]

Salles FT, Merritt RC Jr, Manor U, Dougherty GW, Sousa AD et al. (2009) Myosin IIIa boosts elongation of stereocilia by transporting espin 1 to the plus ends of actin filaments. Nat Cell Biol 11:443–450 [PubMed: 19287378]

Schneider ME, Dose AC, Salles FT, Chang W, Erickson FL et al. (2006) A new compartment at stereocilia tips defined by spatial and temporal patterns of myosin IIIa expression. J Neurosci 26:10243–10252 [PubMed: 17021180]

Self T, Mahony M, Fleming J, Walsh J, Brown SD et al. (1998) Shaker-1 mutations reveal roles for myosin VIIA in both development and function of cochlear hair cells. Development 125:557–566 [PubMed: 9435277]

Taberner AM, Liberman MC (2005) Response properties of single auditory nerve fibers in the mouse. J Neurophysiol 93:557–569 [PubMed: 15456804]

Vreugde S, Erven A, Kros CJ, Marcotti W, Fuchs H et al. (2002) Beethoven, a mouse model for dominant, progressive hearing loss DFNA36. Nat Genet 30:257–258 [PubMed: 11850623]

Walsh T, Walsh V, Vreugde S, Hertzano R, Shahin H et al. (2002) From flies' eyes to our ears: mutations in a human class III myosin cause progressive nonsyndromic hearing loss DFNB30. Proc Natl Acad Sci U S A 99:7518–7523 [PubMed: 12032315]

Zee DS, Fletcher WA (1996) Disorders of the vestibular system. Oxford University Press, New York

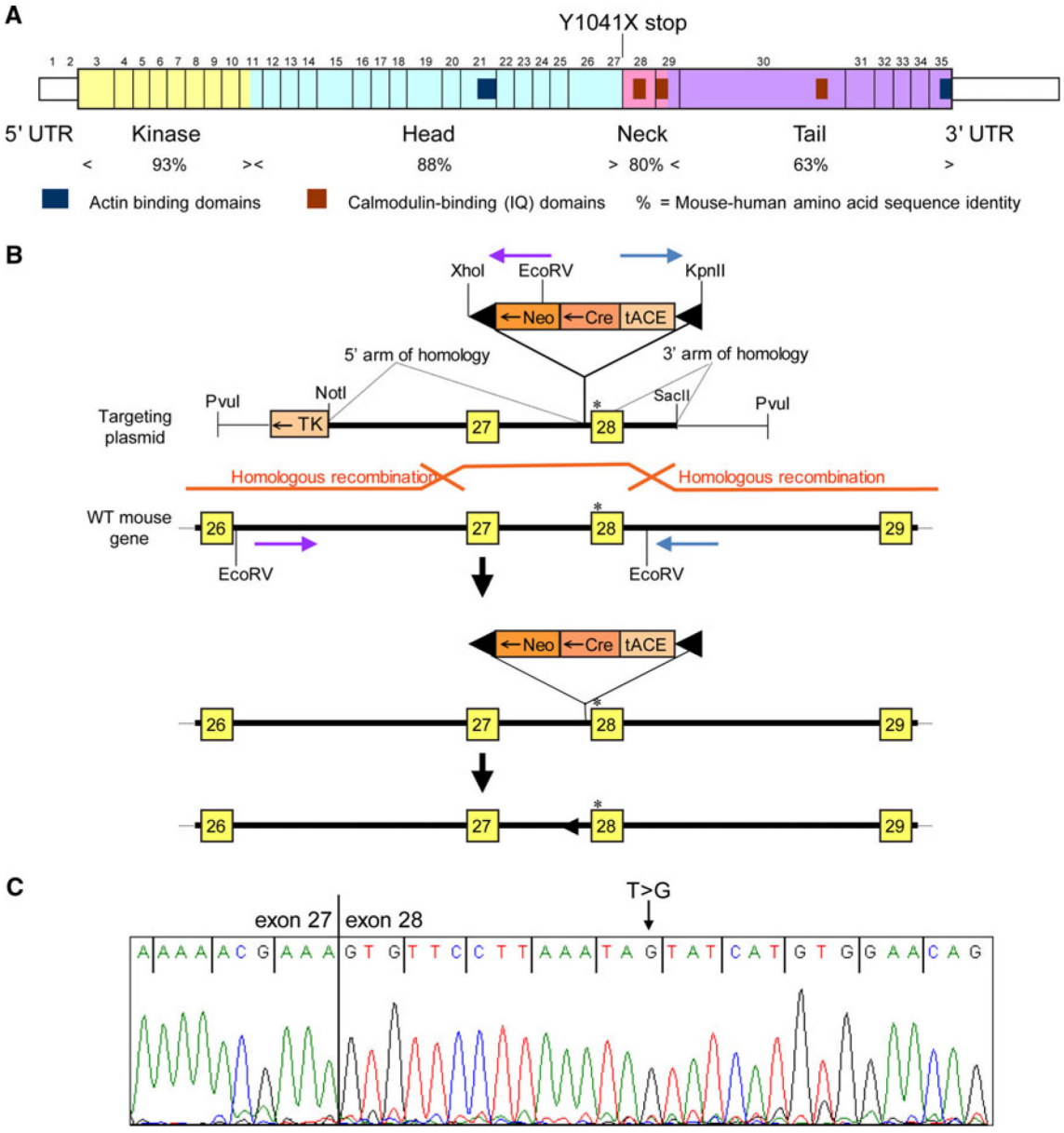

Fig. 1.

The *Myo3a*$^{KI/KI}$ mouse is a model for human adult-onset progressive hearing loss DFNB30. **a** Schematic diagram of the mouse myosin IIIA protein demonstrating the nonsense mutation at mouse Y1041X corresponding to human Y1042X. **b** The targeting construct for the *Myo3a*$^{KI/KI}$ mouse. **c** Sequence of the major RNA transcript from cochlea of homozygous *Myo3a*$^{KI/KI}$ mutant mice

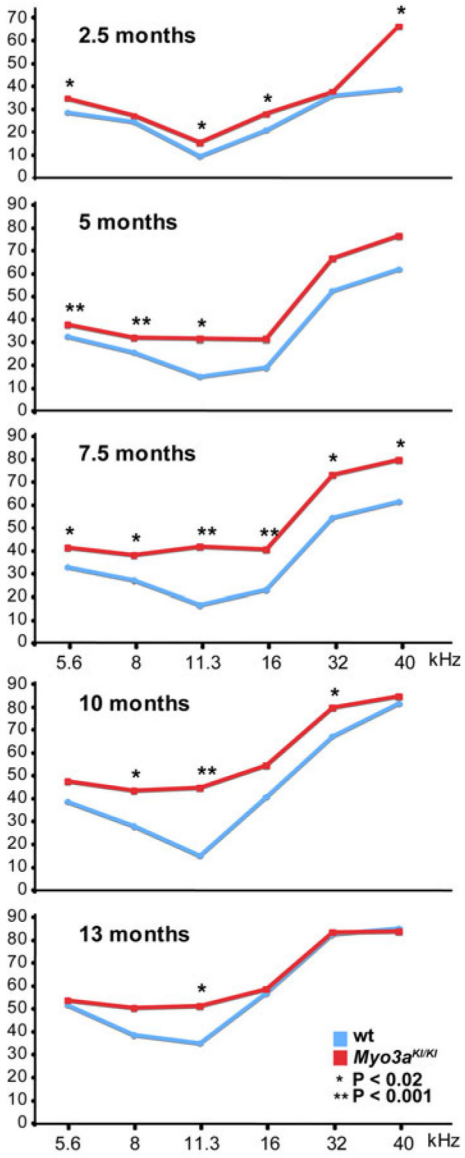

Fig. 2.

Auditory function of mutant and wild-type mice. ABR thresholds of *Myo3a*$^{KI/KI}$ mice at 2.5, 5, 7.5, 10, and 13 months (N = 26). Auditory thresholds of *Myo3a*$^{KI/KI}$ mutant mice (red) and their wild-type littermates (blue) were determined by tone-burst ABR recordings. P values for differences in thresholds between mutant and wild-type mice at each age and frequency are indicated by asterisks. ABR thresholds for all mice at all ages and frequencies are given in Supplementary Table 1. In contrast to wild-type mice, *Myo3a*$^{KI/KI}$ mutant mice showed progressive hearing loss

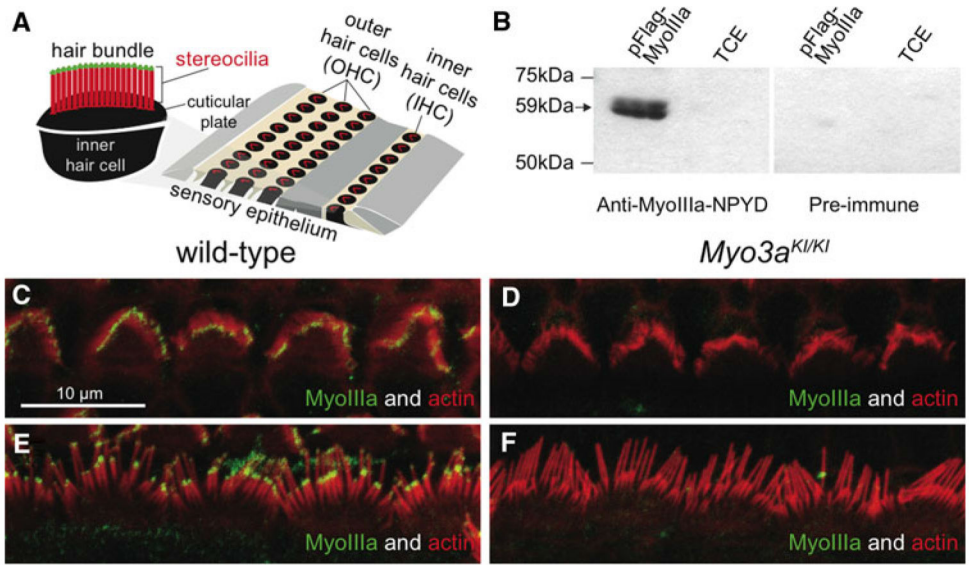

Fig. 3.

Localization of myosin IIIA in the mouse inner ear. **a** Schematic representation of the organ of Corti, showing three rows of outer hair cells (OHCs) and one row of inner hair cells (IHCs), flanked by various types of supporting cells. The hair bundle of an OHC shows the actin-based stereocilia organized in a staircase. **b** The specificity of the custom-made MyoIIIa-NPYD antibody was examined by transfection of HEK293T cells with a construct expressing the pFlag-MyoIIIa tail portion, compared to nontransfected total cell extract (TCE). The antibody detected only myosin IIIA in transfected cells. **c–f** Localization of myosin IIIA in the inner ear. Myosin IIIA (green) is detected at the stereocilia tip in a whole-mount preparation at postpartum day p8, in the outer (**c**) and inner (**e**) hair cells of wild-type mice. Myosin IIIA is not detected in the outer (**d**) and inner (**f**) hair cells of *Myo3a*$^{KI/KI}$ mutant mice. Filamentous actin is labeled with rhodamine/phalloidin (red). *Scale bars* 10 µm

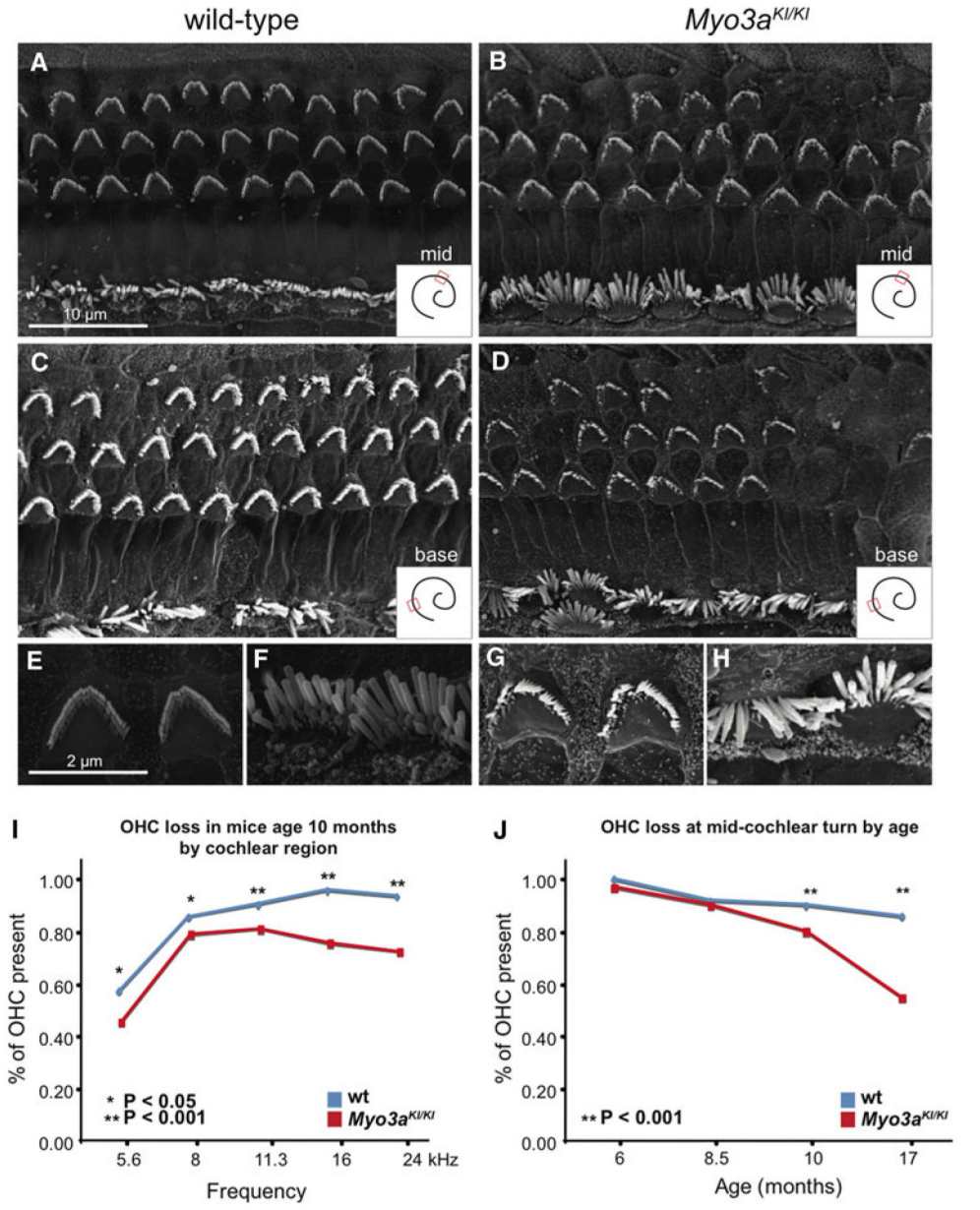

Fig. 4.

Loss of outer hair cells in *Myo3a*$^{KI/KI}$ mutant mice. **a–h** Scanning electron micrographic (SEM) images illustrating hair bundle morphology of 10-month old wild-type mice (**a**, **c**, **e**, **f**) and *Myo3a*$^{KI/KI}$ mice (**b**, **d**, **g**, **h**). Staircase structures of the stereocilia of OHC (**e**, **g**) and IHC (**f**, **h**) are shown at higher magnification. Hair cell loss can be seen in the mutant mice (**b**, **d**). Images were taken from the middle turn (**a**, **b**) and more basal turn (**c**, **d**) of the cochlea. Scale bar = 10 µm for A–D and 2 µm for D–H. **i**, **j** Patterns of hair cell loss in *Myo3a*$^{KI/KI}$ mutant mice. Hair cell loss was determined by counting OHCs in adjacent SEM images. For all panels, cochlear location was used to estimate cochlear frequency (Taberner and Liberman 2005)